DOI: https://doi.org/10.15407/rpra27.04.299
UDC 539.1.08; 539.1.078
PACS: 07.57.Pt

E.A. Alekseev [1,2,3], V.V. Ilyushin [1,2], and R.A. Motiyenko [3]

[1] Institute of Radio Astronomy, National Academy of Sciences of Ukraine
4, Mystetstv St., Kharkiv, 61002, Ukraine
E-mail: ealekseev@rian.kharkov.ua
[2] V.N. Karazin National University of Kharkiv
4, Svoboda Sq., Kharkiv, 61022, Ukraine
E-mail: ilyushin@rian.kharkov.ua
[3] Univ. Lille, CNRS, UMR 8523-PhLAM-Physique des Lasers, Atomes et Molécules
Bât. P5-59 655, Villeneuve d'Ascq Cedex, F-59000 Lille, France
E-mail: roman.motiyenko@univ-lille.fr

SQUARE-WAVE FREQUENCY MODULATION IN MICROWAVE SPECTROSCOPY

Subject and Purpose. *The frequency modulation (FM) combined with lock-in detection, the technique which is used in microwave spectroscopy for enhancing the sensitivity of measurements, as well as the effects due to standing waves in the measuring absorption cell can lead to distortions in the spectral line shapes observed. To ensure the highest possible accuracy derivable from the experimental data, these distortions need to be taken into account. A way of improving the accuracy is to approximate to the experimental line contour with a theoretical line shape that would account for the observable distortion effects. The relevant literature sources suggest examples of theoretical expressions for the line shape in the case of a sinusoidal frequency modulation. This work has been aimed at deriving similar expressions for the case of a square-wave frequency modulation that shall allow increasing the accuracy of measurements.*

Methods and Methodology. *The square-wave-FM signals are obtained with the aid of a direct digital frequency synthesizer that can provide switching between two frequencies known to a high accuracy. This technical solution permits generating FM signals with precisely specified parameters.*

Results. *A closed-form expression has been suggested, based on numerically evaluated line shape derivatives, which allows taking into consideration the basic types of distortions encountered in the spectral line records. The cases that have been considered concern a variety of experimental conditions, including sub-Doppler measurements with Lamb-dip observations.*

Conclusions. *The approach that has been proposed allows one to properly take into account the distortions of spectral line shapes resulting from the use of a square-wave-FM signal, as well as those due to standing wave effects in the spectrometer cell. As has been found, application of this approach to experimental spectra with a variety of modulation parameters permits reducing the errors of frequency determination to* $\pm$ *0.001 MHz, provided the signal-to-noise ratios are reasonably high.*

Keywords: *microwave spectrometer, millimeter-wave spectrum, measurement accuracy, spectral lines.*

Citation: Alekseev, E.A., Ilyushin, V.V., and Motiyenko, R.A., 2022. Square-wave frequency modulation in microwave spectroscopy. *Radio Physics and Radio Astronomy*, **27**(4), pp. 299—311. https://doi.org/10.15407/rpra27.04.299
Цитування: Алєксеєв Є.А., Ілюшин В.В., Мотієнко Р.А. Прямокутна частотна модуляція в мікрохвильовій спектроскопії. *Радіофізика і радіоастрономія*. 2022. Т. 27. № 4. С. 299—311. https://doi.org/10.15407/rpra27.04.299

Introduction

The high resolution microwave spectroscopy which has had a major impact on many important fields of science and technology is an extremely powerful tool for experimental studies of molecular properties [1]. In the process of its development, the microwave spectroscopy has incorporated a number of emerging technologies with the aim of improving frequency measurement accuracy, sensitivity, resolution, and frequency range coverage. The frequency modulated radiation from a source, combined with lock-in harmonic detection represents one of the techniques which have become the classics of microwave spectroscopy, suggesting an efficient way of sensitivity enhancement [2].

The direct digital synthesis method is one of the modern emerging technologies which quite recently has found its application in microwave spectroscopy [3–5]. In modern millimeter and submillimeter wave spectrometers it is common to use a frequency synthesizer referenced to an atomic (usually rubidium) frequency standard, thus providing a basis for high accuracy measurements of spectral line central frequencies (see e.g. [6—9]). As has been shown, the direct digital synthesizer (DDS) can be used, with appropriate filtering provisions, as a reference frequency synthesizer, even in systems with high frequency multiplication factors [3, 4]. Moreover, modern DDSs are capable of providing fast switching between several selected frequencies with continuously varying phases without any overshoots, thus enabling a square-wave frequency modulation (FM) whose parameters are known with a very high precision.

Whereas application of the FM technique provides sensitivity enhancement, it also leads to modulation distortions in the spectral line shapes observed. In the first approximation, the application of FM and lock-in detection may be presented as recording of the first or second (depending on the harmonic selected in lock-in detection) frequency derivative of the true lineshape. Deviations of the recorded line contour from the analytical derivative of the true lineshape depend on the parameters of the FM signal (e.g., the modulation depth). It is just these deviations that we will consider, for the purposes of this paper, as modulation distortions, concentrating on second-order effects in lineshape modifications caused by application of the FM and lock-in detection. One more reason for lineshape distortions is the fact that the molecular gas being investigated is contained, in the course of laboratory measurements, inside the limited space of an absorption cell. As has been shown by Pickett [10], reflections from the cell windows not only produce standing waves within the volume but may also give an asymmetric contribution to the line shapes observed (the so called standing wave distortions). To achieve the highest possible accuracy and resolution out of an experiment, both kinds of distortions should be correctly taken into account in the theoretical line shape expressions to be used as approximate represetations of the experimental spectral records.

Nowadays the sub-Doppler spectroscopy with Lamb-dip observation is widely applied in order to improve spectral resolution and accuracy of transition frequency measurements [11—14]. However, such measurements are also affected by the modulation and standing wave distortions. These distortions have a smaller impact on the measurement accuracy, since the Lamb-dip width has a significantly lower value than the Doppler width for a molecular spectral line. Nevertheless, it is still necessary to take both kinds of distortions into account, in order to reach the highest possible measurement accuracy.

In the literature dedicated to microwave spectroscopy, the issue of theoretical representation of line shape distortions is rather well elaborated for the case of a sinusoidal FM signal (see, e.g. [15]). To the best of our knowledge, Karplus [16] was the first author who has considered (back in 1948) application of the FM in microwave spectroscopy. The issue was further investigated in a number of works (see for example [15, 17]). For the sine-wave-FM signal, the relevant theoretical expressions that allow taking into account both the modulation-produced distortions and the standing wave effect for different lineshape types (e.g. Doppler, Lorentz, Voigt, Galatry, etc.) were finally developed [18]. Unlike the sinusoidal FM, the square-wave-FM is much less studied with regard to distortions in the line contours observed. As appears, application of the square-wave-FM was considered only in Karplus' paper [16], being limited to the simplest case of a Lorentzian lineshape and low frequency square-wave modulation. Also, the standing wave-produced distortions were not considered.

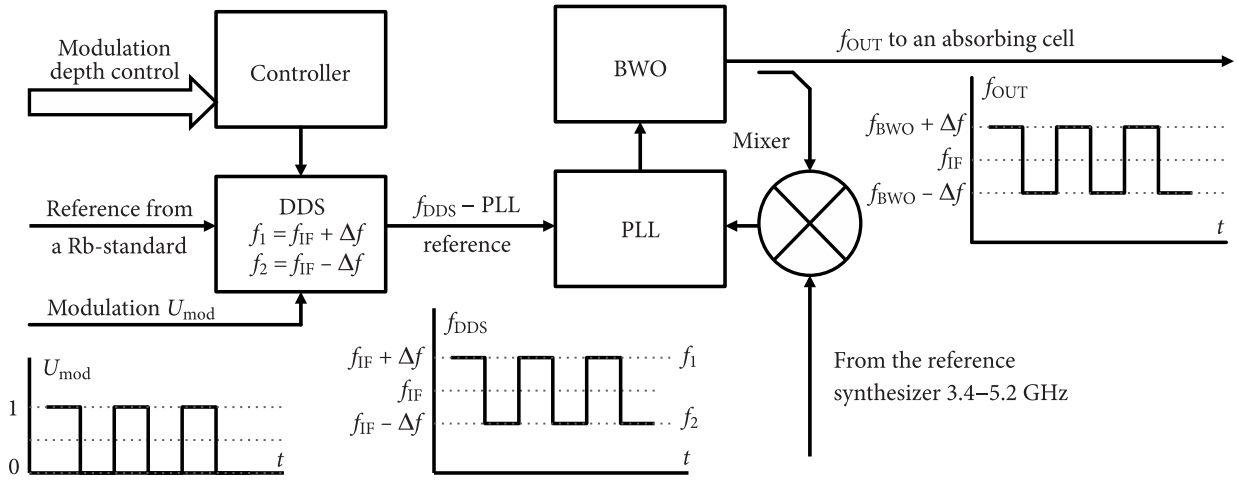

Fig. 1. Formation of a square-wave frequency modulated microwave signal

In this work, we present a new (and relatively economic computationally) approach to the line shape analysis which is suitable in the case of the square-wave-FM. The approach takes into account both the modulation-produced and the standing wave effects in the case of a Doppler-limited resolution, as well as the sub-Doppler resolution measurements. In addition, we describe an implementation of a DDS-based square-wave-FM system as it has been realized in the millimeter-wave spectrometer of the Institute of Radio Astronomy, NAS of Ukraine. Also, we demonstrate application of the new approach to processing of experimental records.

1. Experimental details: DDS-based square-wave frequency modulation

All the test measurements we have used to demonstrate our new approach to line shape analysis were obtained with the automated synthesizer-based millimeter-wave spectrometer of the Institute of Radio Astronomy, NAS of Ukraine. The instrument is a conventional absorption spectrometer, a general description of which can be found in Ref. [8]. In this subsection we would like to discuss, for the sake of presentation completeness, the approach we normally use for generating microwave square-wave-FM signals.

The proposed solution which is implemented in our millimeter wave spectrometer [8] is shown schematically in Fig. 1. The probe signal which is fed into an absorbing cell is provided by a backward wave oscillator (BWO). The frequency at the BWO output is stabilized by a phase locking loop (see the PLL in Fig. 1). The idea of the modulation scheme is based on applying a frequency modulated reference signal to the PLL. Since the PLL supports a pre-defined offset between the reference and the stabilized signal, the BWO output also becomes frequency modulated. The required FM reference is formed by a DDS which is programmed by a controller (Fig. 1) to set two frequency profiles, f_1 and f_2. The modulating signal (represented in terms of logic levels) simply switches the DDS frequency output between these two values. Thus, the PLL reference is generated as a frequency shift keying signal. In order to ensure proper parameters for the FM signal, the values of f_1 and f_2 are chosen as follows.

Let us designate the offset PLL operating frequency (in the absence of any modulation) as f_{IF}. The modulation depth Δf is chosen in accordance with experimental conditions. In order to perform measurements within a wide frequency range with a Doppler-limited resolution, as well as with a sub-Doppler one, the modulation depth Δf may be selected from among the values 1, 2, 4, 8, 16, 32, 64, or 128 kHz. The actual modulation depth Δf is programmed by the logic signals of modulation depth control (see Fig. 1). The frequency profiles are chosen as $f_1 = f_{IF} + \Delta f$ and $f_2 = f_{IF} - \Delta f$, and the modulation signal U_{mod} (logic) just switches the DDS output between these two values. The switching frequency F_{mod} may be selected within the (1.5 to 21.0) kHz range (depending on experimental conditions). Since the DDS reference signal is formed, based on a rubidium frequency standard, both of the frequencies f_1 and f_2 are known to a very high ac-

curacy. Accordingly, the parameters of the DDS FM signal are also known to a high accuracy. The signal obtained in such a way is applied as a reference for the PLL which provides for phase stabilization of the BWO output. Owing to the frequency modulated reference, the BWO output will be also frequency modulated, effectuating switching between the $f_{\mathrm{OUT1}} = f_{\mathrm{BWO}} + \Delta f$ and $f_{\mathrm{OUT2}} = f_{\mathrm{BWO}} - \Delta f$ frequencies. Obviously, a FM signal like that is affected by the PLL response. However, as has been shown in [5], this influence is negligible.

It should be noted that the majority of modern millimeter- and submillimeter-wave FM spectrometers operate with sine-wave frequency modulation. This is because the commercially available frequency synthesizers serving as reference-signal sources for the spectrometers involve built-in sine-wave modulators. To a certain degree, it is because of this fact that the methods developed so far for processing the experimentally obtained data are based on an assumption of sine-wave-FM signals. The sine-wave-FM signal normally is generated through continuous variation of the synthesizer frequency, such that there is no time interval within the modulation period where the frequency could be regarded as fixed. This means that only crude estimates can be suggested for parameters of the signal. In contrast, the square-wave-FM implies switching between two frequencies known to a high accuracy. In addition, the application of modern DDSs enables such switching with a continuous phase without any overshoots. This is the reason why application of the square-wave-FM produced by a DDS allows us to generate an FM signal with parameters known to a high level of accuracy.

2. Line shape distortions due to standing wave

Consider the distortions in the contours of molecular spectral lines associated with the standing waves in the absorbing cell of a spectrometer. We will need this information for deriving a general expression used for processing the recorded spectra, including the modifications due to the FM. The central frequencies of the spectral lines are determined by means of a least-square fit of an experimental record with an appropriate function. Let us denote the proper lineshape function with a central frequency ν_0, as $\alpha(\nu, \nu_0)$. Also, let $i_0(\nu)$ denote the transfer function of an empty absorbing cell that takes into account the frequency dependences from the source and the detector, as well as the reflections (standing waves) inside the cell. The detector current $i(\nu)$ caused by the radiation passing through the absorbing cell of effective length l may be expressed, according to the Beer–Lambert–Bouguer law, as

$$i(\nu) = i_0(\nu)\exp(-\alpha(\nu,\nu_0)l) = i_0(\nu)(1-\alpha(\nu,\nu_0)l). \quad (1)$$

(Assuming a low amount of absorption this could be expanded in a Taylor series, retaining just the linear term.)

It should be noted that the presence of reflections in an absorption cell leads to baseline variations and may cause certain problems, such as sensitivity and accuracy limitations. These problems may require being considered in detail. Because of source frequency modulation and lock-in detection the spectra are recorded, in the first approximation, as a frequency derivative of the line's contour (here we suppose the first harmonic detection). The first frequency derivative of Eq. (1) will be

$$i'(\nu) = i_0'(\nu) - i_0'(\nu)\alpha(\nu,\nu_0)l - i_0(\nu)\alpha'(\nu,\nu_0)l. \quad (2)$$

Within the zeroth order approximation, it is supposed that the baseline varies only very slowly, hence $i_0(\nu)$ may be taken to be constant in a close vicinity of the line, thus suggesting $i_0'(\nu) = 0$. So, the two first terms in Eq. (2) are usually set to be zeros. Now, $\alpha'(\nu,\nu_0)$ is a symmetric function with respect to ν_0 (see, for example, the expressions for either Doppler or Lorentz line shapes). Therefore, by means of approximating to the spectral record, represented here by $i'(\nu)$ with a symmetric function (e.g., either Gaussian or Lorentzian) one can obtain an accurate estimate for the central frequency ν_0. However, generally $i_0(\nu)$ is not a constant magnitude, mainly because of reflections (standing wave manifestations) in the absorbing cell, and therefore it is necessary to make account of all terms in Eq. (2). It should be noted that although $i_0(\nu)$ is affected by frequency dependent traits of the radiation source and the detector, the variations due to the standing waves are the most rapid and significant ones within a close vicinity of the spectral line (which is taken into account in the approximating representation of a particular line contour). Using the analytical derivative $\alpha'(\nu,\nu_0)$ as

an approximate form of the line contour (modified through application of the FM and lock-in detection) we follow the procedure further on referred to as the "analytical derivative" approach.

In reality, even with a moderate level of reflections in the absorbing cell, the standing wave variations may be comparable in magnitude with the strongest lines in the molecular spectrum and much larger than the spectral variations caused by the absorption due to weak lines. To facilitate the spectrum assignment process, some filtering of the standing wave variations is normally performed at the initial stage of processing of the recorded spectrum (using, for instance, the Savitsky and Golay smoothing [19]). The variations remaining after this filtering of the background may be expressed, in a close proximity around the line center, as a linear function of frequency, *viz.* $d(\nu-\nu_c)+p$. Here ν_c is the central frequency of the spectral region being processed in the vicinity of the considered line; if needed, we can in fact use a quadratic or even a cubic polynomial here. This polynomial will correspond to the first term of Eq. (2). If there were no second term in Eq. (2), the line contour would still be symmetric with respect to the residual baseline represented by the term $d(\nu-\nu_c)+p$. However, the second term of Eq. (2) contains a small contribution from the initial lineshape which destroys the symmetry of the observed line contour. The main problem here is that *a priori* the relative importance of the second and the last term in Eq. (2) is unknown. To overcome this difficulty, we propose to include their ratio to the list of parameters to be fitted and determine it from the asymmetry of the line contour observed. Let us denote this ratio as *r*, then the lineshape approximating function $S(\nu,\nu_0)$ may be expressed as

$$S(\nu,\nu_0)=d(\nu-\nu_c)+p+r\alpha(\nu,\nu_0)+\alpha'(\nu,\nu_0). \qquad (3)$$

Thus, in the course of spectrum record processing we will also determine, in addition to parameters of the line shape function $\alpha(\nu,\nu_0)$, the parameters *d* and *p* of the linear function which takes into account the residual baseline variations in a close proximity around the line center, as well as the parameter *r*, making account of the line shape distortions due to reflections in the absorbing cell.

The proposed approach performs data treatment in the frequency domain and allows taking into account the line shape distortions due to standing waves. It should be noted that a time domain analysis of standing wave-produced distortions in the sine-wave-FM signal was considered in [15]. Compared with paper [15], the approach proposed here is simpler computationally and, in addition, can be expanded rather easily to the case of the square-wave FM.

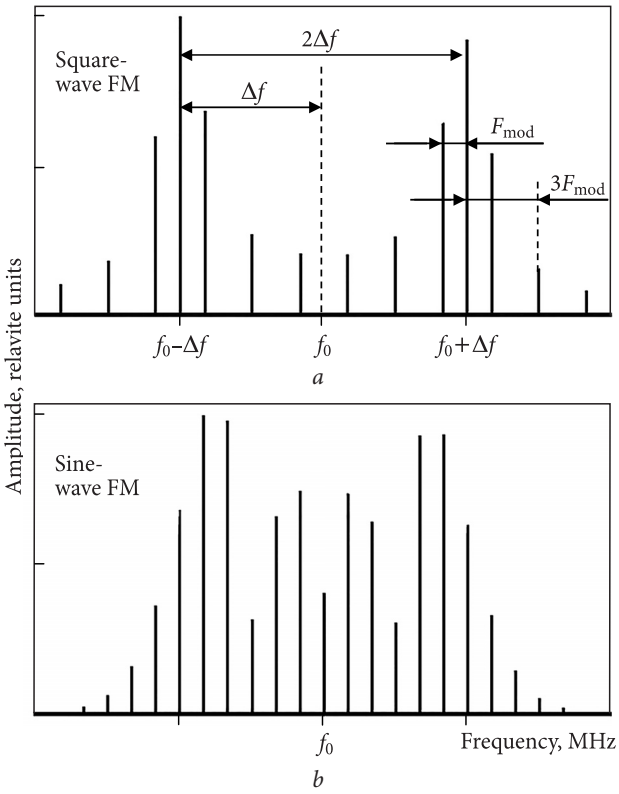

Fig. 2. Sample spectra of square-wave- and sine-wave-frequency modulated signals

3. Line shape modification due to square-wave-FM

As has been mentioned, the spectrometer operates with a FM source of radiation. A frequency — modulated signal with a carrier f_0 is characterized by the modulation frequency F_{mod} and modulation depth Δf. Usually, Δf is chosen to be considerably greater than F_{mod}. Consider now some features of the square-wave FM signal whose simulated spectrum, with $\Delta f / F_{\text{mod}} = 6$, is shown in Fig. 2. First of all, the spectrum contains only odd harmonics of the modulation frequency F_{mod} (see Fig. 2, *a*). The absence of even harmonics suggests that the lock-in detector should operate at the first harmonic of the modulation frequency. For comparison, in Fig. 2, *b*, a spectrum of a sine-wave-FM signal with the same

modulation depth (amplitude of frequency variation) is shown. It is evident that the spectrum of the square-wave-FM signal is rather different from the usual sine-wave-FM one. This difference should be taken into account for a proper analysis of the line shapes observed.

As can be seen from Fig. 2, the square-wave-FM signal contains two intense components shifted by $\pm\Delta f$ from the central frequency f_0. With some level of approximation, these two components allow us to replace an analytical expression for the line shape derivative by its numerically calculated approximate form. The molecular spectrum is recorded by means of a step-by-step source frequency scanning. At each frequency point, the lock-in detector measures the difference between two values on the line contour corresponding to the two strongest spectral components of the source. This gives the numerical value of the line shape derivative with the digitization interval of $2\Delta f$. Therefore, in the case of a square-wave- FM signal as the numerically calculated derivative of the line shape the following expression may be applied:

$$\alpha'(\nu,\nu_0)=\frac{\alpha(\nu+\Delta f,\nu_0)-\alpha(\nu-\Delta f,\nu_0)}{2\Delta f}. \qquad (4)$$

By combining Eq. 3 and Eq. 4 the approximating function for the line contour processing may be finally expressed as follows:

$$S(\nu,\nu_0)=d(\nu-\nu_c)+p+r\alpha(\nu,\nu_0)+ \\ +\frac{\alpha(\nu+\Delta f,\nu_0)-\alpha(\nu-\Delta f,\nu_0)}{2\Delta f}. \qquad (5)$$

We would like to remind that the linear term $d(\nu-\nu_c)+p$ with fitted parameters d and p compensates baseline variations in a close proximity of the line center ν_0. The term $r\alpha(\nu,\nu_0)$ takes standing wave distortions into account, with r being a fitted parameter. Modulation depth Δf is preset at the stage of measurements and during the fit this parameter is known and fixed at the experimental value. Actual form of the lineshape function $\alpha(\nu,\nu_0)$ is chosen depending on the experimental conditions.

Application of Eq. (5) to line contour approximation in the course of spectrum record processing constitutes the essence of proposed in this work approach. For convenience, we will call our approach as "numerical derivative" approach (basing on the way the modulation line shape modifications are represented in Eq. (5)). This naming convention is also selected to underline an opposition to "analytical derivative" approach with which we compare our new approach.

4. Low pressure case: Doppler-limited resolution

One of the simplest cases corresponds to the Doppler-limited resolution measurements performed at a rather low pressure of molecular gas in the absorbing cell. Our tests for the OCS molecule have shown that this regime is achieved with the molecular gas sample pressures of order of 10^{-6} bar. Under such experimental conditions the observed line shape is described with the Gaussian function:

$$\alpha(\nu,\nu_0)=G(\nu,\nu_0)=A\exp\left(-\ln 2\frac{(\nu-\nu_0)^2}{(\Delta\nu_D)^2}\right), \qquad (6)$$

where A is the amplitude of the line, ν_0 is the central frequency, and $\Delta\nu_D$ is the Doppler linewidth. The final expression for the approximation function is obtained by combining Eq. (6) and Eq. (5):

$$S(\nu,\nu_0)=d(\nu-\nu_c)+p+rG(\nu,\nu_0)+ \\ +\frac{G(\nu+\Delta f,\nu_0)-G(\nu-\Delta f,\nu_0)}{2\Delta f},$$

where $d,p,r,A,\nu_0,\Delta\nu_D$ are the fitted parameters. Parameter Δf is preset at the stage of measurements and it is fixed during the fit.

In order to test the proposed approach, we recorded, with a Doppler-limited resolution, the $J=5-4$ transition of the OCS molecule with different modulation parameters and standing wave distortions. The standing wave distribution was changed by means of displacement of the receiving horn in the spectrometer. Sample pressure in the absorbing cell was kept as low as approximately 10^{-6} bar that allowed us to reach Doppler limited resolution corresponding to the Gaussian lineshape. Modulation parameters (modulation depth Δf) were varied within the wide range from $\Delta f=2$ kHz to $\Delta f=128$ kHz. Some typical examples of recorded lines with corresponding line contour approximations are shown in Fig. 3. Note that relatively low signal-to-noise ratio observed for some records of the OCS line (which is in fact rather intense) at Fig. 3 is a consequence of a combination of the rather low pressure with the small Δf values.

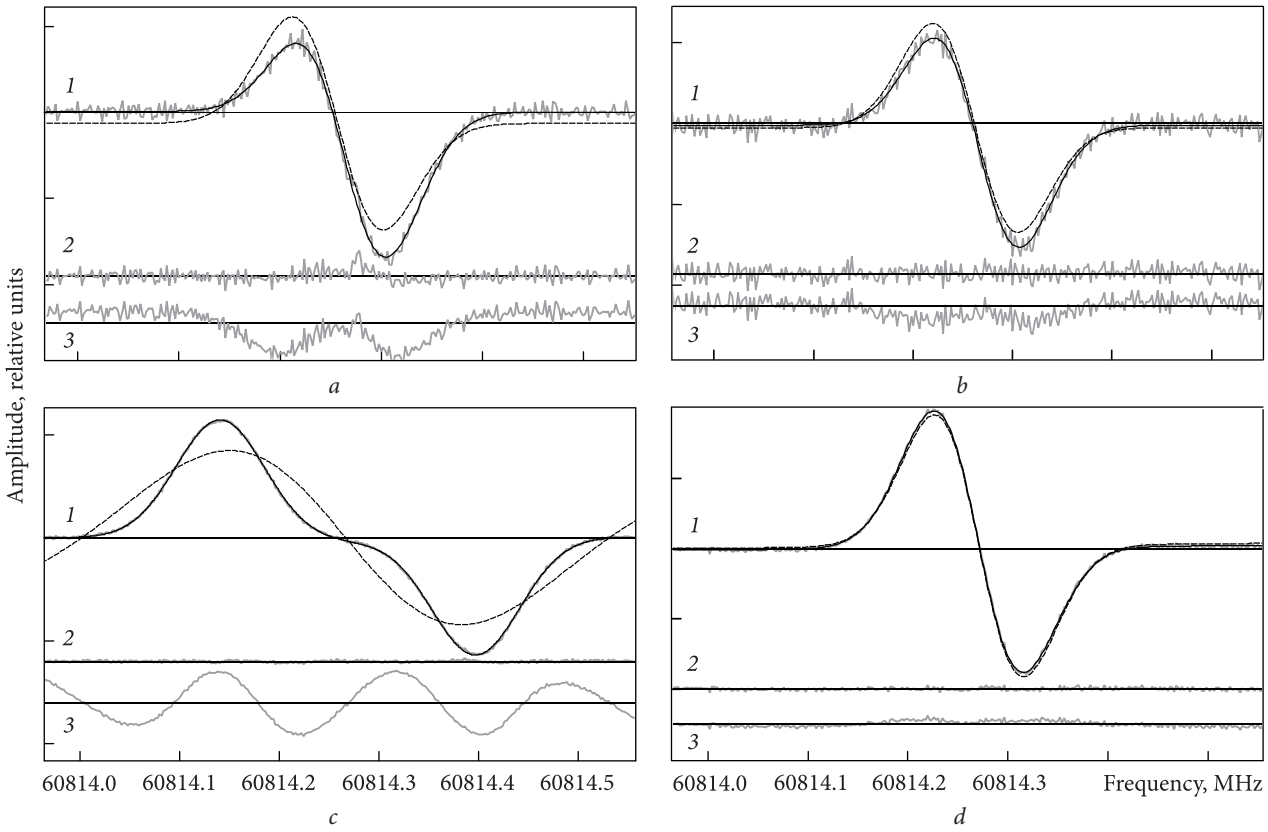

Fig. 3. Records of the $J = 5–4$ transition of the OCS molecule obtained with different distribution of standing wave in the absorbing cell and with different modulation depths (see text for further details). In all figures amplitude is in relative units

The measured transition frequency for this line is $\nu_{\mathrm{OCS}} = 60\,814.2691(5)$ MHz. This value was obtained by averaging all our measurements which characterized by a good signal-to-noise ratio for this line.

In Fig. 3, the gray solid line *1* represents corresponding experimental record of the OCS line. In the same place, the black solid line is the result of approximation obtained using the proposed new approach. For comparison, the black dash line gives the result of approximation which employs analytical derivative of the Gaussian line shape function. The analytical derivative of the line shape function doesn't take possible asymmetry of the line contour due to standing wave effect as well as modulation distortions caused by the finite value of the modulation depth into account. The larger value of the modulation depth we use in our experiment the larger difference is observed between the "analytical derivative" and "numerical derivative" approaches, with the most illustrative example given at Fig. 3, *c*. Line *2* represents the residuals of the fit for the "numerical derivative" approach, while line *3* gives the residuals for the "analytical derivative" approach.

Central line frequencies obtained from the least squares approximation using both approaches described above for a number of spectrum records with different modulation and standing wave conditions are collected in Table. For the convenience of further discussion, the numbering of the rows is given in the first column of Table. Columns 2 and 3 of Table contain the values of central line frequency ν_{exp} and corresponding residual $\nu_{\mathrm{exp}} - \nu_{\mathrm{OCS}}$ obtained using the "analytical derivative" approach. Columns 5 and 6 give the same information obtained using the "numerical derivative" approach. Columns 4 and 7 give approximation results for the Doppler width parameter $\Delta\nu_D$ obtained, respectively, with the "analytical" and "numerical" approaches.

The measurement results of Table may be divided into three groups. Group one (rows from 1 to 7) presents results for the spectral records showing a significant asymmetry due to the standing wave effect. These are illustrated by Fig. 3, *a* and Fig. 3, *b* corresponding to rows 2 and 6 of Table. As can be seen, our approach provides a good fit to the line contours, whereas the "analytical derivative" approach fails to

reproduce the asymmetry observed. As a result, the deviations from the averaged value ν_{OCS} are of the order of 1 kHz (see column 6) within the "numerical derivative" approach, while in the case of an "analytical derivative" the deviations observed reach values up to 12 kHz (see column 3). Thus, the "numerical derivative" approach allows reducing the errors of frequency determination at least by an order of magnitude.

Group two (rows from 8 to 10, emphasized with **bold** script), presents results for the spectral records obtained with rather high modulation-caused distortions. An example of such a record is given in Fig. 3, *c* (it corresponds to row 9 of Table). It is seen that the "analytical derivative" approach is not capable of reproducing the line contour observed, whereas fitting with the use of the "numerical derivative" approach demonstrates a very nice quality of approximation (Fig. 3, *c*, curve *2*). Again, for the "numerical derivative" approach the deviations from the average value are of the order of 1 kHz (see column 5), which demonstrates capability of the technique to correctly take into account even significant modulation-produced distortions.

Group three (rows from 11 to 23, given in *italic*) presents results for the recorded spectra which can be reproduced rather well with either one of the approaches. These are the records for which neither the modulation, nor the standing wave-produced distortions are that significant. An example of one such record is presented in Fig. 3, *d*. From the modulation point of view, it means that the modulation depth is lower than the spectral line width. In what concerns the standing waves, it corresponds to the case when the line position coincides with either a maximum or a minimum of the standing wave existing in the absorbing cell (thus making the $i_0'(\nu)$ term in Eq. (2) close to zero and removing the asymmetry-caused contribution from the line contour). While in this

Results of measurements of the OCS $J = 5$—4 transition frequency

Row number	"Analytical derivative" approach, MHz			"Numerical derivative" approach, MHz		
	ν_{exp}	$\nu_{\mathrm{exp}} - \nu_{\mathrm{OCS}}$	$\Delta\nu_d$	ν_{exp}	$\nu_{\mathrm{exp}} - \nu_{\mathrm{OCS}}$	$\Delta\nu_d$
1	2	3	4	5	6	7
1	60814.2620	–0.0071	0.0627	60814.2704	0.0013	0.0501
2	60814.2569	–0.0122	0.0637	60814.2683	–0.0008	0.0514
3	60814.2609	–0.0082	0.0640	60814.2693	0.0002	0.0515
4	60814.2595	–0.0096	0.0647	60814.2689	–0.0002	0.0514
5	60814.2647	–0.0044	0.0636	60814.2692	0.0001	0.0521
6	60814.2626	–0.0065	0.0607	60814.2675	–0.0016	0.0502
7	60814.2652	–0.0039	0.0622	60814.2679	–0.0012	0.0515
8	**60814.2656**	**–0.0035**	**0.1828**	**60814.2680**	**–0.0011**	**0.0513**
9	**60814.2666**	**–0.0025**	**0.1815**	**60814.2688**	**–0.0003**	**0.0519**
10	**60814.2670**	**–0.0021**	**0.1868**	**60814.2691**	**0.0000**	**0.0519**
11	*60814.2678*	*–0.0013*	*0.0616*	*60814.2684*	*–0.0007*	*0.0506*
12	*60814.2708*	*0.0017*	*0.0615*	*60814.2697*	*0.0006*	*0.0511*
13	*60814.2708*	*0.0017*	*0.0627*	*60814.2690*	*–0.0001*	*0.0509*
14	*60814.2710*	*0.0019*	*0.0617*	*60814.2691*	*0.0000*	*0.0510*
15	*60814.2711*	*0.0020*	*0.0631*	*60814.2698*	*0.0007*	*0.0514*
16	*60814.2687*	*–0.0004*	*0.0668*	*60814.2690*	*–0.0001*	*0.0506*
17	*60814.2679*	*–0.0012*	*0.0867*	*60814.2690*	*–0.0001*	*0.0513*
18	*60814.2690*	*–0.0001*	*0.0876*	*60814.2698*	*0.0007*	*0.0525*
19	*60814.2700*	*0.0009*	*0.0642*	*60814.2700*	*0.0009*	*0.0523*
20	*60814.2700*	*0.0009*	*0.0679*	*60814.2697*	*0.0006*	*0.0517*
21	*60814.2712*	*0.0021*	*0.0619*	*60814.2699*	*0.0008*	*0.0512*
22	*60814.2703*	*0.0012*	*0.0621*	*60814.2694*	*0.0003*	*0.0505*
23	*60814.2701*	*0.0010*	*0.0678*	*60814.2700*	*0.0009*	*0.0516*

case both approaches give rather similar results (as can be seen from columns 3 and 6 of Table), still the "numerical derivative" approach demonstrates somewhat smaller deviations from the averaged value $\nu_{\mathrm{OCS}} = 60\,814.2691(5)$ MHz.

It should be noted that in routine measurements performed with our spectrometer, both the standing wave-conditioned and the modulation-produced distortions lead to frequency determination errors up to ±10 kHz, even at a low level of reflections in the absorbing cell. By carefully adjusting the standing wave's distribution (by means of displacing the reception horn in the spectrometer) we can reduce this error down to 1 kHz. However, that would require an enormous amount of time since each line should be adjusted individually. The proposed approach allows us to solve the standing wave problem without tedious manual adjustments of the spectrometer configuration and to reduce the frequency determination error down to ±1 kHz for a rather strong isolated spectral line.

Finally, let us discuss the approximation results for the Doppler width parameter $\Delta\nu_D$ as obtained within both approaches. The Doppler line width may be calculated using the well-known expression [20]:

$$\Delta\nu_D = \frac{\nu_0}{c}\sqrt{\frac{2NkT\ln 2}{M}} = 3.575\times10^{-7}\sqrt{\frac{T}{M}}\nu_0, \qquad (7)$$

where T is temperature (K); M is molar mass of the molecule (g/mol); ν_0 the spectral line's central frequency (MHz); N the Avogadro number; k the Boltzmann constant, and c is the velocity of the radiation (usually this is the speed of light). For the OCS line at $\nu_{\mathrm{OCS}} = 60\,814.2691(5)$ MHz we obtained the value of $\Delta\nu_D = 0.0486$ MHz (assuming $T = 300$ K). It is seen from the 7th column of Table that the "numerical derivative" approach gives nearly the same value of $\Delta\nu_D$ for all measurements, irrespective of the modulation and standing wave conditions, and the value is rather close to the theoretical prediction provided by the above given expression. We attribute the discrepancy of several kHz between experiment and theory to the residual effects of collisional broadening, in particular due to collisions with the cell walls. As concerns the "analytical derivative" approach, it is seen from the 4th column of Table 1 that the fitted results for $\Delta\nu_D$ are far from being satisfactory, especially for the second group of measurements that demonstrated significant modulation distortions. Thus, we may conclude that the "numerical derivative" approach gives an opportunity to properly separate the additional broadening of the observed lines that is due to modulation effects.

5. Intermediate pressure case: Voigt profile

In routine investigations of molecular spectra the low pressure regime is not employed because it may significantly limit intensities of the observed lines. Usually, higher pressures are applied in the experiments in order to provide for balance between spectral resolution (limited by line broadening) and measurement sensitivity (note that higher sample pressures mean larger numbers of molecules that interact with the radiation). In the most common case, the contributions from the Doppler-line broadening and the collisional broadening are of comparable orders of magnitude. Accordingly, in the first-order approximation the observed line shape can be described by Voigt's profile which is a convolution of the Gaussian and the Lorentzian function [21],

$$V(\nu,\nu_0) = \\ = A\frac{\sqrt{\ln 2}(\Delta\nu_L)}{\pi^{3/2}(\Delta\nu_D)}\int_{-\infty}^{+\infty}\frac{\exp[-\ln 2(t/\Delta\nu_D)^2]}{(\nu-\nu_0-t)^2+(\Delta\nu_L)^2}\,dt.$$

Analytical expression for Voigt function contains integration which complicates its application. As is known, the numerical convolution process is computationally rather expensive. For this reason a number of approximations of the Voigt function that are more convenient computationally were proposed, e.g. [21—23]. We will apply an efficient analytical approximation for the Voigt function described in [22].

In order to obtain an approximating function for spectrum record processing let us substitute the expression for Voigt's profile into Eq. (5) :

$$S(\nu,\nu_0) = d(\nu-\nu_c)+p+rV(\nu,\nu_0)+ \\ +\frac{V(\nu+\Delta f,\nu_0)-V(\nu-\Delta f,\nu_0)}{2\Delta f}, \qquad (8)$$

where the parameters to be fitted are $d, p, r, A, \nu_0, \Delta\nu_L$. The parameter $\Delta\nu_D$ is fixed at the calculated value level as obtained with the use of the theoretical expression for the Doppler linewidth [20] (see Eq. 7 in the previous section). The Δf parameter is preset

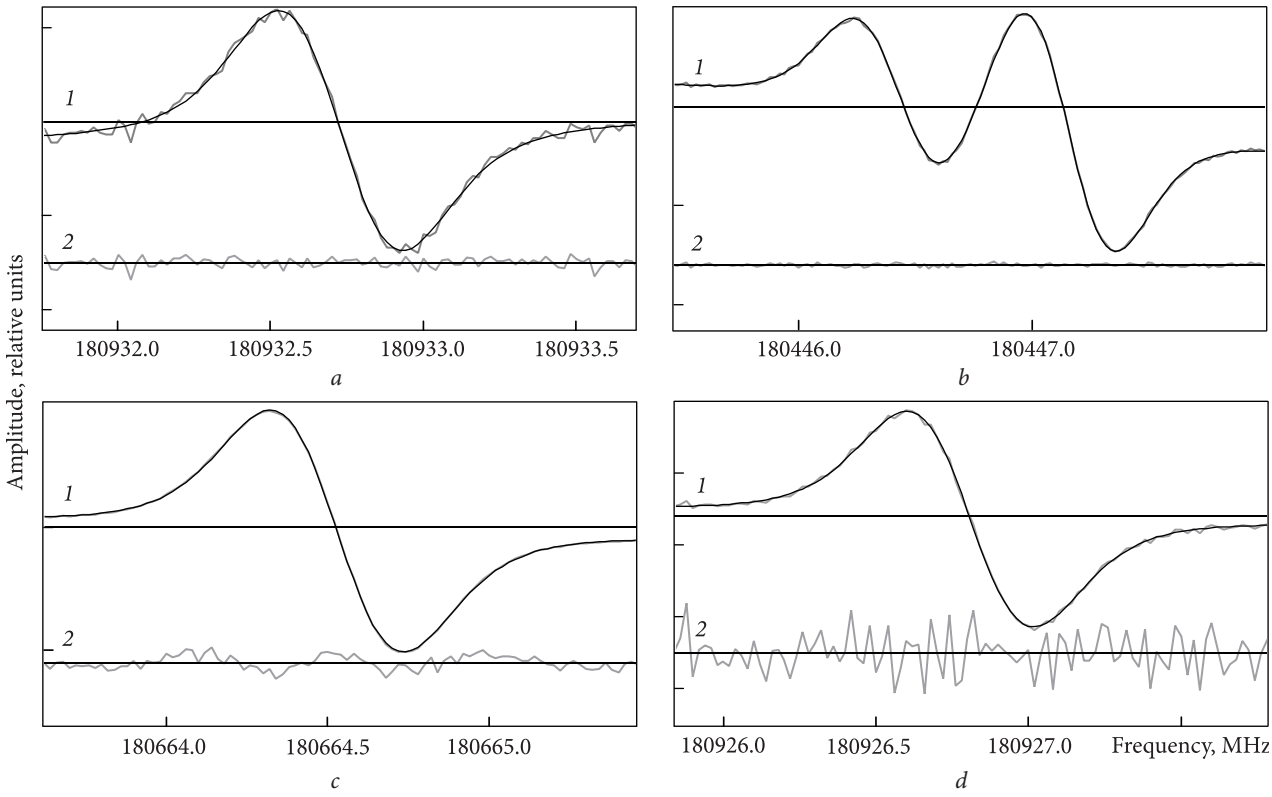

Fig. 4. Records of several dimethyl ether lines and the corresponding approximations obtained within the "numerical derivative" approach with Voigt's line shape function. The amplitudes are expressed in relative units throughout

at the stage of measurements, and hence is also kept fixed during the fitting process.

In Fig. 4 we present the records of several spectral lines belonging to the dimethyl ether molecule, and the corresponding approximations derived within the "numerical derivative" approach. The gray solid line *1* represents the experimental record and the black solid line nearby demonstrates the result of applying the "numerical derivative" approach. Line *2* represents the residual between experiment and approximation. A typical record for an isolated line is presented in Fig. 4, *a*. As follows from the residual between experiment and approximation, the proposed approach ensures a good fit to the observed line contour. In Fig. 4, *b* we show an example of two adjacent lines with slightly overlapping contours. The extension of the model to the case of two lines processed simultaneously is quite obvious; we just add to Eq. (8) a new Voigt function with a central frequency and amplitude of its own. Again the residual between experiment and approximation demonstrated in Fig. 4, *b* represents just noise. Thus, we can conclude that the Voigt profile calculated with the use of the analytical approximation of Ref. [22] (in combination with the "numerical derivative" approach) offers satisfactory results and proves to be applicable for line contour approximations in the case where contributions from the Doppler and the collisional line broadening mechanisms are comparable.

It should be noted that more sophisticated line shape functions are known, which take into account higher-order physical effects such as speed changing collisions that may lead to the so-called Dicke narrowing, or the dependence of collisional relaxation rates upon molecular velocities. Among such models one can refer to the speed dependent Voigt profile or the Galatry profile [18]. Consideration of these line shape functions is appropriate when the lines with a high signal-to-noise ratio are observed and deviations from the Voigt profile become evident (see e.g. [18]). An example of such case is presented in Fig. 4, *c* where the residuals for the fit using Voigt profile are scaled by a factor of 10 and we see some oscillating deviation from a straight line for the residual between experiment and approximation. Fig. 4, *d*, which presents a weaker line with residuals also scaled by a factor of 10, illustrates the fact that such oscillating deviation may indeed be

observed only in the case of a rather high signal-to-noise ratio. It is obvious from the two above considered cases (Doppler's and Voight's profiles) that our "numerical derivative" approach does not impose any restrictions on the line shape functions for $\alpha(\nu,\nu_0)$. At the same time, for a majority of the spectral lines observed the Voigt profile function gives rather good results, which is the reason why we do not consider in this paper application of more sophisticated (and more computationally expensive) model functions.

6. Sub-Doppler spectroscopy with Lamb-dip observation

The Lamb-dip observation is a powerful tool for enhancing the spectral resolution and measurement accuracy [11—14]. When this technique of achieving sub-Doppler spectral resolution is applied the line contour may be considered as a Lamb-dip record observed against the background of a Doppler broadened line. The Lamb-dip contour may be well represented by the Lorentz function:

$$L(\nu,\nu_0)=\frac{B}{(\nu-\nu_0)^2+(\Delta\nu_L)^2}, \tag{9}$$

where B is the amplitude of the Lamb-dip, and $\Delta\nu_L$ is the width of the Lamb-dip. In the simplest case, assuming an absence of the hyperfine structure of the transition, the Lamb-dip record should be fitted to a sum of both the Gauss and Lorentz functions, each having the same central frequency but an amplitude of its own (combining Eq. (6) and Eq. (9)):

$$\alpha(\nu,\nu_0)=G(\nu,\nu_0)+L(\nu,\nu_0). \tag{10}$$

Then final expression of the function for line shape approximation in the case of sub-Doppler resolution measurements with Lamb-dip observation is obtained by combining Eq. (10) with Eq. (5):

$$S(\nu,\nu_0)=d(\nu-\nu_c)+p+r\Big[L(\nu,\nu_0)+G(\nu,\nu_0)\Big]+ \\ +\frac{L(\nu+\Delta f,\nu_0)-L(\nu-\Delta f,\nu_0)}{2\Delta f}+ \\ +\frac{G(\nu+\Delta f,\nu_0)-G(\nu-\Delta f,\nu_0)}{2\Delta f}, \tag{11}$$

where fitted parameters are the following d, p, r, A, B, ν_0, $\Delta\nu_D$, $\Delta\nu_L$. As previously, the parameter Δf is preset at the stage of measurements and it is fixed during the fit. In the case when multiple Lamb dips are resolved the model is extended by adding to the expression (11) of required quantity of Gauss and Lorentz terms with their own central frequencies and amplitudes.

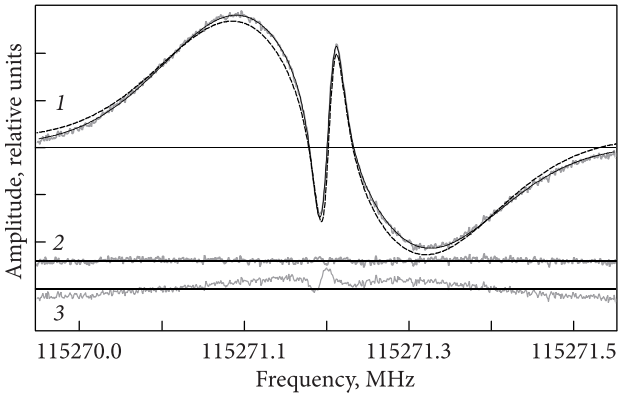

Fig. 5. The Lamb dip record of the $J = 1 \leftarrow 0$ transition of the CO molecule (gray solid line). Black solid line *1* is the result of approximation of the record using the "numerical derivative" approach. Black dashed line represents the approximation with the "analytical derivative" approach (standing wave effects are not taken into account). Curve *2* gives the residual for the proposed "numerical derivative" approach (contains mainly noise). Curve *3* gives the residual of the fit that does not take the influence of standing wave in the cell into account

Expression (11) was applied for the fitting of the Lamb-dip record of the CO molecular line presented in Fig. 5. Here, the experimental record and the result of approximation are shown with gray and black solid lines respectively. For comparison, "analytical derivative" which doesn't take standing wave and modulation distortions into account is shown with the dash line. The residuals for the two types of approximation are also given in Fig. 5 (curve *2* for the "numerical derivative" approach and curve *3* for the "analytical derivative" approach). It is evident that the agreement between experiment and approximation is very good for the "numerical derivative" approach and have noticeable problems in the case of the "analytical derivative" approach. Such problems in Lamb-dip approximation may increase the frequency determination error up to several kHz.

Thus, the proposed "numerical derivative" approach gives a considerable improvement of the fit quality, which allows us to minimize frequency determination errors and to improve the spectral resolution by a proper account for the additional broadening caused by modulation effects. It should be noted that owing to a very small width of a Lamb-dip

the modulation distortions may be quite noticeable even for a rather low modulation depth. Although the proposed approach takes large modulation distortions into account, in order not to hamper the resolution of the Lamb-dip technique we are choosing the value of the full modulation depth $2\Delta f$ to be not larger than the full width of the Lamb-dip. The frequency of the $J = 1 \leftarrow 0$ CO rotational transition obtained using the "numerical derivative" approach is 115 271.2022(5) MHz. This value is in a good agreement within a confidence interval with previously measured value of 115 271.2018(5) MHz [11].

Conclusions

The application of direct digital synthesizers in microwave spectroscopy allows implementing the square-wave-FM technique with modulation parameters known to a high accuracy. To take the full advantage of this technical solution we have introduced an improved theoretical model for spectral record processing. The model proposed allows taking into account both the distortions owing to reflections in the absorbing cell and the modulation-produced distortions resulting from application of a square-wave-FM signal. As has been shown, this new approach may be equally well applied in the cases of Doppler limited spectral resolution, sub-Doppler resolution measurements with a Lamb-dip technique, and routine measurements when the Doppler and the collisional broadening effects are of comparable orders of magnitude. Our experimental tests suggest that with the new approach the frequency determination error may be reduced to ±0.001 MHz for the lines recorded with moderate signal-to-noise ratios.

Acknowledgments. *E. Alekseev gratefully acknowledges financial support from Centre National de la Recherche Scientifique (CNRS, France) and from Université de Lille (France).*

REFERENCES

1. De Lucia, F.C., 2010. The submillimeter: A spectroscopist's view. *J. Mol. Spectrosc.*, **261**(1), pp. 1—17. DOI: https://doi.org/10.1016/j.jms.2010.01.002.
2. Nagourney, W., 1978. Baseline suppression in microwave spectroscopy frequency modulation and harmonic detection. *Rev. Sci. Instrum.,* **49**, pp. 1072—1076. DOI: 10.1063/1.1135516.
3. Alekseev, E.A., Zakharenko, V.V., 2004. Direct digital synthesizer as a reference source of a millimeter-wave frequency synthesizer. In: *Proc. V Int. Kharkov Symp. "Physics and engineering of millimeter and submillimeter waves"*. Kharkov, Ukraine, 21—26 June 2004, pp. 782—784. DOI: 10.1109/MSMW.2004.1346148.
4. Alekseev, E.A., Zakharenko, V.V., 2007. Direct Digital Synthesizer at the Microwave Spectroscopy. *Radio Phys. Radio Astron.*, **12**(2), pp. 205—214 (in Russian).
5. Alekseev, E.A., 2011. Direct Digital Frequency Synthesizers: Potentialities and Limitations for Microwave Spectroscopy Applications. *Radio Phys. Radio Astron.*, **2**(4), pp. 369—378. DOI: 10.1615/RadioPhysicsRadioAstronomy.v2.i4.100.
6. Zakharenko, O., Motiyenko, R.A., Margulès, L., Huet, T.R., 2015. Terahertz spectroscopy of deuterated formaldehyde using a frequency multiplication chain. *J. Mol. Spectrosc.*, **317**, pp. 41—46. DOI: http://dx.doi.org/10.1016/j.jms.2015.09.005.
7. Alekseev, E.A., Motiyenko, R.A., Margulès, L., 2012. Millimeter- and Submillimeter-Wave Spectrometers on the Basis of Direct Digital Frequency Synthesizers. *Radio Phys. Radio Astron.*, **3**(1), pp. 75—88. DOI: 10.1615/RadioPhysicsRadioAstronomy.v3.i1.100.
8. Alekseev, E.A., Ilyushin, V.V., Mescheryakov, A.A., 2014. High-Precision Microwave Spectrometer with Sub-Doppler Spectral Resolution. *Radio Phys. Radio Astron.*, **19**, pp. 364—374 (in Russian). DOI: https://doi.org/10.15407/rpra19.04.364.
9. Daly, A.M., Kolesniková, L., Mata, S., Alonso, J.L., 2014. The millimeter and submillimeter wave spectrum of *cis*-methyl vinyl ether. *J. Mol. Spectrosc.*, **306**, pp. 11—18. DOI: https://doi.org/10.1016/j.jms.2014.10.003.
10. Pickett, H.M., 1980. Determination of collisional linewidths and shifts by a convolution method. *Appl. Optics. Roy. Soc. London*, **19**(16), pp. 2745—2749. DOI: 10.1364/AO.19.002745.
11. Winnewisser, G., Belov, S.P., Klaus, Th., Schieder, R., 1997. Sub-Doppler measurements of the rotational transitions of carbon monoxide. *J. Mol. Spectrosc.*, **184**(2), pp. 468—472. DOI: 10.1006/jmsp.1997.7341.
12. Cazzoli, G., Puzzarini, C., Stopkowicz, S., Gauss, J., 2010. Hyperfine structure in the rotational spectra of trans-formic acid: Lamb-dip measurements and quantum-chemical calculations, *Astron. Astrophys.*, **520**, id. A64. DOI: 10.1051/0004-6361/201014787.
13. Melosso, M., Dore, L., Gauss, J., Puzzarini, C., 2020. Deuterium hyperfine splittings in the rotational spectrum of NH_2D as revealed by Lamb-dip spectroscopy. *J. Mol. Spectrosc.*, **370**, id. 111291. DOI: https://doi.org/10.1016/j.jms.2020.111291.
14. Belov, S.P., Golubiatnikov, G.Yu., Lapinov, A.V., Ilyushin, V.V., Alekseev, E.A., Mescheryakov, A.A., Hougen, J.T., and Li-Hong Xu, 2016. Torsionally mediated spin-rotation hyperfine splittings at moderate to high J values in methanol. *J. Chem. Phys.*, **145**, id. 024307. DOI: https://doi.org/10.1063/1.4954941.
15. Dore, L., 2003. Using Fast Fourier Transform to compute the line shape of frequency-modulated spectral profiles. *J. Mol. Spectrosc.*, **221**(1), pp. 93—98. DOI: https://doi.org/10.1016/S0022-2852(03)00203-0.

16. Karplus, R., 1948. Frequency modulation in microwave spectroscopy. *Phys. Rev.*, **73**(9), pp. 1027—1034. DOI: https://doi.org/10.1103/PhysRev.73.1027.
17. De Vreede, J.P.M., Gillis, M.P.W., Dijkerman, H.A., 1988. Linewidth, Lineshift, and Lineshape Measurements on Rotational Transitions of OCS Using Frequency Modulation. *J. Mol. Spectrosc.*, **128**(2), pp. 509—520. DOI: https://doi.org/10.1016/0022-2852(88)90166-X.
18. Nguyen, L., Buldyreva, J., Colmont, J.-M., Roharth, F., Wlodarczak, G., Alekseev, E.A., 2006. Detailed profile analysis of millimetre 502 and 602 GHz N_2O-$N_2(O_2)$ lines at room temperature for collisional linewidth determination. *Mol. Phys.*, **104**(16–17), pp. 2701—2710. DOI: https://doi.org/10.1080/03067310600833534.
19. Savitzky, A., Golay, M.J.E., 1964. Smoothing and Differentiation of Data by Simplified Least Squares Procedures. *Anal. Chem.*, **36**(8), pp. 1627—1639. DOI: https://doi.org/10.1021/ac60214a047.
20. Gordy, W., Cook, R.L., 1984. *Microwave Molecular Spectra*. New York: John Wiley & Sons. ISNB 0471086819.
21. Di Rocco, H.O., 2005. The exact expression of the Voigt profile function. *J. Quant. Spectrosc. Radiat. Transf.*, **92**, pp. 231—237. DOI: https://doi.org/10.1016/j.jqsrt.2004.08.002.
22. McLean, A.B., Mitchell, C.E.J., Swanston, D.M., 1994. Implementation of an efficient analytical approximation to the Voigt function for photoemission lineshape analysis. *J. Electron Spectrosc. Relat. Phenom.*, **69**, pp. 125—132. DOI: https://doi.org/10.1016/0368-2048(94)02189-7.
23. Di Rocco, H.O., Cruzado, A., 2012. The Voigt Profile as a Sum of a Gaussian and a Lorentzian Functions, when the Weight Coefficient Depends Only on the Widths Ratio. *Acta Phys. Pol. A*, **122**, pp. 666—669. DOI: 10.12693/APhysPolA.122.666.

Received 11.09.2022

Є.А. Алєксеєв [1,2,3], В.В. Ілюшин [1,2], Р.А. Мотієнко [3]

[1] Радіоастрономічний інститут Національної академії наук України
вул. Мистецтв, 4, Харків, 61002, Україна
E-mail: ealekseev@rian.kharkov.ua
[2] Харківський національний університет імені В.Н. Каразіна
майдан Свободи, 4, Харків, 61022, Україна
E-mail: ilyushin@rian.kharkov.ua
[3] Лабораторія фізики лазерів, атомів та молекул (ФЛАМ), Лілльський університет
Bât. P5-59 655 Villeneuve d'Ascq Cedex, F-59000 Lille, France
E-mail: roman.motiyenko@univ-lille.fr

ПРЯМОКУТНА ЧАСТОТНА МОДУЛЯЦІЯ В МІКРОХВИЛЬОВІЙ СПЕКТРОСКОПІЇ

Предмет і мета роботи. Техніка частотної модуляції (ЧМ) у поєднанні з синхронним детектуванням, що використовується для підвищення чутливості в мікрохвильовій спектроскопії, а також ефекти стоячої хвилі в поглинальній кюветі призводять до спотворень форми спостережуваних спектральних ліній. Щоб отримати з експерименту дані найвищої точності, ці спотворення мають бути враховані. Підвищення точності можна здійснити шляхом апроксимації експериментального контуру лінії за допомогою теоретичної форми лінії, що враховує спостережувані спотворення. У літературі наводяться детально розроблені теоретичні вирази для форми лінії в разі синусоїдальної ЧМ. Метою роботи є розробка відповідних виразів для сигналу з прямокутною ЧМ, що дозволять підвищити точність вимірювань.

Методи та методологія. Для отримання сигналу прямокутної ЧМ було застосовано синтезатор прямого цифрового синтезу частоти, котрий забезпечував перемикання між двома частотами, що відомі з високою точністю. Таке рішення дозволило генерувати ЧМ-сигнал із прецизійно заданими параметрами.

Результати. Запропоновано вираз, що базується на чисельно отриманій похідній від форми лінії, котрий здатен враховувати основні типи спотворень записів спектральних ліній. Розглянуто випадки різних експериментальних умов, включно з субдоплерівськими вимірюваннями зі спостереженням провалу Лемба.

Висновок. Запропонований підхід дозволяє належним чином ураховувати спотворення форми спектральних ліній, що виникають при застосуванні прямокутної ЧМ, а також під впливом стоячої хвилі у вимірювальній кюветі. Застосування такого підходу до експериментальних записів спектра з різними параметрами модуляції показало, що для ліній, отриманих із суттєвим значенням співвідношення сигнал/шум, похибки визначення частоти можуть бути зменшені до ±0.001 МГц.

Ключові слова: *мікрохвильовий спектрометр, міліметровий спектр, точність вимірювань, спектральні лінії.*